Photoinduced Surface Trapping and the Observed Carrier Multiplication Yields in Static CdSe Nanocrystal Samples

Marco Califano*

Institute of Microwaves and Photonics, School of Electronic and Electrical Engineering, University of Leeds, Leeds LS2 9JT, United Kingdom

ABSTRACT Photocharging has been suggested recently as the explanation for the spread of carrier multiplication yields reported by different groups. If this hypothesis can be plausible in the case of PbSe, it is inconsistent with the reported experimental data relative to CdSe nanocrystals and cannot therefore explain the large discrepancies found in that material system between static and stirred samples. An alternative explanation, photoinduced surface trapping, is suggested here, based on the results of atomistic semiempirical pseudopotential calculations of the Auger recombination rates in a number of excitonic configurations including a variety of surface traps, which show that the photoinduced surface trapping of the hole, which leaves the core negatively charged (but the nanocrystal neutral overall), can lead to recombination rates that are indistinguishable from those of a conventional biexciton with four core-delocalized carriers and therefore result in exaggerated CM yields in static samples. In contrast, the recombination rate of a charged exciton is found to be at least a factor of 2.3 smaller than that of the biexciton and therefore easily distinguishable from it experimentally. Although increased trapping at surface states was dismissed as unlikely for PbSe nanocrystals, in the case of CdSe, this hypothesis is further supported by much experimental evidence including recent spectroscopic measurements on CdSe nanostructures, single-nanocrystal photoionization studies on CdSe core/shell nanocrystals, and state-resolved transient absorption studies of biexcitonic states, all showing increased probability of surface trapping for highly excited states. These results suggest that multicarrier processes could be mediated by different mechanisms in CdSe and PbSe nanocrystals.

KEYWORDS: CdSe nanocrystals · Auger processes · carrier multiplication · surface states · pseudopotential method

One of the most complex, and still poorly understood, aspects relative to semiconductor nanocrystals (NCs) is the characterization of their surface. It is known that some ligands only partially passivate the surface dangling bonds,[1−3] allowing the presence of intrinsic trap states, whereas other capping groups introduce themselves trap states of various depths, depending on their electronegativity.[4] A surface-state-related broad feature was found to the red of the main emission peak in both photoluminescence (PL)[5,6] and electrogenerated chemiluminescence[7] spectra, which optically detected magnetic resonance studies[8] assigned to deep hole traps. The growth of shells of various thicknesses is known to modify the surface properties, in many cases removing most trap states and generally improving the surface quality, as testified by the observation of increased PL quantum yields and decreased emission intermittency (blinking),[9] although surface-state emission was also found in CdSe/ZnSe core/shell NCs.[10] This inorganic passivation is nevertheless also known[8] to introduce defects at the interface due to the lattice mismatch that may occur between core and shell material. Many fundamental questions, however, remain unanswered, such as the nature and dynamics of the interactions of (multi-) exciton states with surface ligands, interface defects, and the surrounding solvents. Particularly relevant to the recent debate on the origin of the wide spread of reported carrier multiplication (CM) yields estimates is the extent to which the presence of surface states affects the efficiency of the Auger recombination (AR) process. The presence of multiple electron−hole pairs following a CM event is, in fact, revealed by a ∼10−100 ps fast decay component in the nanocrystal population dynamics, due to fast AR of the multiexciton, whereas a ∼10 ns slow component is associated with the presence of a single electron−hole pair decaying radiatively. As the efficiency of CM is directly linked to the ratio of the signal amplitude in these two regimes,[11,12] it is important to identify whether the presence of trap states can affect the observed AR times and hence potentially interfere with the accuracy of the measured CM yields.

A recent paper[13] suggested photoinduced charging of the NCs as an explanation for the discrepancies in the CM yields

* Address correspondence to m.califano@leeds.ac.uk.

Received for review December 7, 2010 and accepted April 14, 2011.

Published online April 14, 2011
10.1021/nn200723g

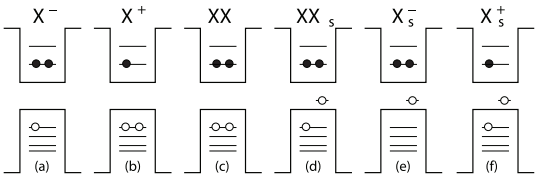

Figure 1. Schematics of the different excitonic configurations considered in this work: conventional negative (a) and positive (b) trions, and biexciton (c); biexciton (d), negative (e), and positive (f) trions with a hole trapped in a surface state. The configuration in (d) represents a possible alternative to a "negative trion" (a) where the NC is neutral overall due to the presence of a hole localized on the surface.

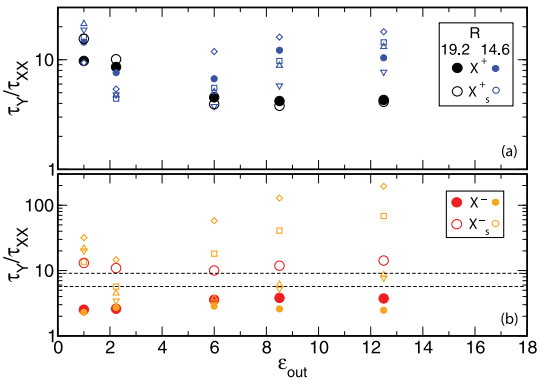

Figure 2. AR lifetimes in units of τ_{XX}, calculated as a function of the dielectric constant of the NC environment ε_{out} for negative (X^-, red and orange symbols) and positive (X^+, black and blue symbols) trions where the carriers are either all delocalized in the dot core (solid symbols) or where one hole is trapped in one of the four surface states considered (t_1, squares; t_2, diamonds; t_3, up-triangles; t_4, down-triangles; T_1 circles). The symbols are also size-coded: large symbols are relative to the R = 19.2 Å NC, whereas smaller ones to the R = 14.6 Å NC. The black dashed lines indicate the upper and lower limit for the negative trion lifetimes estimated experimentally in R > 25 Å NCs.[21]

reported in the literature. The authors show that in PbSe, while the early PL decay of stirred samples can be fitted to a *bi*-exponential curve with time constants consistent with tri- and biexciton Auger recombination lifetimes, static samples exhibit a *tri*-exponential PL decay that combines the neutral biexciton lifetime with two additional distinct time scales that they attribute to the decay of a charged multiexciton and a trion (a charged exciton, Figure 1a,b). The discrepancies in the reported CM yields are therefore attributed to unintentional (photoinduced) charging of the NCs which would have led to an overestimate of the CM efficiency in older measurements, but which would have been removed in the stirred samples used in more recent experiments, where more modest yields were observed in similarly sized NCs. This hypothesis, if plausible for PbSe NCs, does not however explain the observed spread of CM yields in CdSe NCs where, in the case when CM was detected,[14] transient absorption time traces at low pump intensity and high photon energies exhibited (i) a *bi*- (not *tri*-) exponential decay (where τ_1 was equal to the single exciton lifetime), with (ii) the magnitude of the fast component τ_2 essentially identical to that of the relaxation constant measured at high excitation intensities for photon energies below the CM threshold (where therefore the probability of photoionization was very low), which was also consistent with the data reported in earlier sets of experiments.[15] Since a later transient PL experiment[12] on similarly sized CdSe NC samples at similar excitation energies did not find any evidence of CM, according to the photocharging hypothesis, the CM-like signatures detected in ref 14 should have been due entirely to NC charging. If this is the case, given the relationship $1/\tau_{XX} = 2/\tau_{X^-} + 2/\tau_{X^+}$,[16] then the observed early time decay components should have been consistent with the Auger recombination times of trions (τ_{X^-} or τ_{X^+}) and therefore different by at least a factor of 2 from (and not the same as) those measured at high fluences and low photon energies, relative to biexcitons. Indeed, such a difference would have been larger than the experimental resolution and therefore easily detectable.

The results presented here show that if in a photoexcited NC a hole is not ejected from the NC but trapped at its surface, *and therefore the NC as a whole is neutral* (Figure 1d), then the AR lifetimes calculated in the presence of that surface state can be essentially the same as those of a NC with four carriers delocalized in the core (Figure 1c). This would explain the discrepancy between the experimental data of Schaller *et al.*[14] and those of Nair and Bawendi[12] in terms of photoinduced surface trapping (PIST) of the hole in the samples during the former set of experiments.[14]

RESULTS AND DISCUSSION

AR lifetimes were calculated for several excitonic complexes (X^+, X^-, and XX) (i) in the presence of charge carriers which are all completely delocalized within the dot core (Figure 1a–c) and (ii) with a photogenerated hole trapped in one range of surface states (Figure 1d–f), from shallower to deeper, in nearly spherical wurtzite CdSe NC with R = 14.6 and 19.2 Å,[17] using semiempirical pseudopotential wave functions[18] and applying the formalism developed in ref 16.

Surface states originating from a variety of different sources, from the capping molecule (externally induced traps) to Se dangling bonds (intrinsic traps), were simulated by unpassivating surface Se atoms according to the procedure detailed in ref 19, where the removal of one passivant from one of the two different types of Se dangling bonds (single and double) from different positions on the NC surface (top, bottom, along or off the wurtzite c axis, and on the NC "equator") created a range of surface states t_i (with i = 1,...,4 increasing with depth, from an energy $\varepsilon_{t_1} \approx \varepsilon_{h_1} + 170$ meV to $\varepsilon_{t_4} \approx \varepsilon_{h_1} + 580$ meV[17] [further details can be found in ref 19]), where the hole has different degrees of overlap with the electron wave function.

Finally, the influence of different environments, including solvents, capping groups, and semiconductor shell materials, was also accounted for in the calculations through the selection of appropriate macroscopic dielectric functions for the system (see Computational Methods below for more details): the results will therefore be plotted (i) for different NC sizes (R = 14.6 and 19.2 Å) and (ii) different surface states (t_i and T_i), (iii) as a function of the matrix dielectric constant ε_{out}.

Figure 2 displays the AR lifetimes (in units of τ_{XX}) calculated as a function of the dielectric constant of the NC environment ε_{out} for positive (panel a) and negative (panel b) trions where two carriers are delocalized within the dot core and the remaining hole is either delocalized (Figure 1b,a) or trapped in one of the four surface states considered (Figure 1f,e). These configurations represent the possible scenarios proposed by McGuire *et al.*[13] to explain the discrepancies in the CM yields reported in the literature: the case of photoinduced charging of the NCs. According to this hypothesis, the CM-like signatures detected in CdSe NCs in ref 14, but not in ref 12, should have been due entirely to NC charging. It is evident, however, that the Auger recombination times of trions shown in Figure 2 differ by at least a factor of 2.3 from those calculated for neutral biexcitons, in a wide range of dielectric environments (hence possible surface terminations and solvents), and therefore, the two cannot be confused (a similar result was recently obtained in the case of InAs NCs[20]). The conclusion is that the presence of photocharged NCs cannot explain the experimental observations in CdSe samples.[14]

The AR lifetimes of negatively charged trions were recently estimated[21] to be a factor of about 5.8−9.2 (dashed lines in Figure 2b) longer than the biexciton lifetime in larger CdSe/CdS core/shell NCs with d > 50 Å. For the sizes considered here, these values would be consistent with the presence of surface-trapped holes in the trions (empty symbols in Figure 2b). This was, however, probably not the case in the samples of ref 21, as a localized hole would have led to much higher radiative lifetimes than those estimated in that work. The calculated ratios τ_{X^-}/τ_{XX} (solid circles in Figure 2b) exhibit an increase with size, especially for large dielectric environments, which suggests a possible compatibility for larger diameters with the above estimates.[21] It has to be noted, however, that the trion lifetimes reported in ref 21 were not measured *directly* but were obtained from nontrivial simulations of tri- or quadri-exponential PL decay curves, which involved a number of parameters in the fitting procedure.

If photocharging cannot explain the data by Schaller *et al.*,[14] a similar mechanism, photoinduced surface trapping, which still involves the ejection of a carrier from the NC *core*, is suggested here as a possible explanation. In this process, following a high energy excitation, the hot photogenerated hole, due to its high kinetic energy, samples regions of the NC very close to the surface, leading to an increased cross section for capture by a surface trap. The possibility of this occurrence in PbSe NCs was discarded by McGuire *et al.*[13] because it contrasted with the observed increase in the amplitude of the early time PL signal. Nevertheless, for CdSe, which, as discussed above, exhibits very different relaxation dynamics, this hypothesis appears to be more realistic. Indeed, an increased probability of surface trapping for highly excited states, with a trapped carrier fraction as high as 60%, was recently found in femtosecond pump−probe spectroscopic measurements on CdSe rods.[22] State-resolved transient absorption studies of biexcitonic states in CdSe NCs[23] also revealed enhanced surface trapping rates for excited exciton states yielding biexcitons constituted by a surface-trapped state and the band edge exciton. Further analysis of the transient features evidenced, moreover, that the majority of surface-trapping-related signals arose from hole (rather than electron) trapping, consistently with previous assignments.[9,26−28] This scenario is further supported by recent single-NC photoionization studies on CdSe core/shell NCs by Li *et al.*,[24] who suggested that high energy excitations can create charge-separated complexes, where the hole is likely to be trapped on the surface and the electron is in a core-delocalized state. Very importantly, they point out[24] that these complexes are not created by low energy, direct excitation of the emitting exciton. Another indication of the occurrence of photoassisted charge trapping in CdSe NCs comes from single-dot blinking studies *in the absence of illumination*,[25] which found an extremely low probability

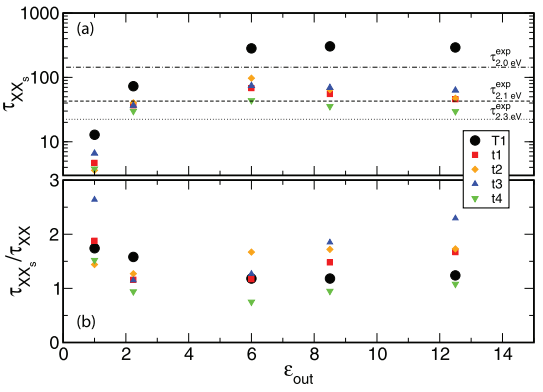

Figure 3. Calculated Auger biexciton recombination lifetimes as a function of the dielectric constant of the NC environment ε_{out} for NCs with first absorption peak position at 2.2 eV (colored solid symbols) and 2.07 eV (black solid circles): in this configuration, two electrons and one hole are delocalized in the dot core and the remaining hole is trapped in one of the four surface states considered (2.2 eV: t_1, red squares; t_2, orange diamonds; t_3, blue triangles; t_4, green triangles; 2.07 eV: T_1, black circles). The black lines indicate the values of the experimental AR decay times[15,26] measured in NCs with a first absorption peak energy equal to 2.3 eV (22 ps, dashed line), 2.1 eV (45 ps, dotted line), and 2.0 eV (147 ps, dash-dotted line) for comparison.

of "on−off" transitions (*i.e.*, transitions from a high quantum yield state to a low quantum yield state, commonly associated with the trapping of a carrier) in the dark.

Upon trapping, the hole excess energy can be transferred either to the lattice or to the photogenerated electron *via* an inverse Auger cooling process,[16,29] as suggested by Frantsuzov and Marcus.[30] In contrast to photoionization, however, in the case of PIST, the NC would remain neutral overall, and according to the results obtained here, the AR rates would be similar to those observed in a biexciton with all core-delocalized carriers, therefore consistent with experiment.[14]

Figure 3 shows the calculated AR times in this configuration (Figure 1d), as a function of the dielectric constant of the environment. In the case of the deepest trap t_4 (green down-triangles), all values of the screening considered yield lifetimes within the experimental range[15,26] (dotted and dashed lines in panel a) and very similar (almost indistinguishable for ε_{out} = 2.238, 8.5, and 12.5) to those of a perfectly passivated NC (see Figure 3b). Similarly, for the large NC, the ratio between the AR lifetimes of XX and XX_s was found to be close to 1 for most values of ε_{out}. These results are in excellent agreement with the experimental data by Pandey and Guyot-Sionnest,[32] who found that the AR lifetimes measured in CdSe NCs treated with hole-trapping surfactants (dodecanethiol) which introduce *deep* hole traps resulting in a low fluorescence quantum yield (QY < 0.2%) were virtually the same as those observed in bright CdSe NCs (with a QY of ∼22%).

The origin of this apparently puzzling behavior is a complex interplay of the following factors: (i) the location and degree of localization of the hole on the surface; (ii) the reduction in the electron−hole wave function overlap caused by the localization of the hole; (iii) the increase in dielectric confinement for large values of ε_{out}; (iv) the reduction in size confinement with increasing NC radius. In the case of a core-delocalized biexciton (*i.e.*, for $h_j = h_1$ in eq 2) both terms on the right-hand side of eq 2a are equal, and the electron contribution τ_e^{-1} to the total AR rate (first term on the right-hand side of eq 1) is larger than the hole contribution τ_e^{-1} (second term on the right-hand side of eq 1), with the ratio τ_h/τ_e exhibiting a strong dependence on both size and external screening. When one of the holes is localized on the surface ($h_j = t_i$), the two components of τ_e^{-1} in eq 2a have different magnitudes: $1/\tau_{X^-}(h_1)$, coming from the recombination of one electron with the core-delocalized hole, is only slightly affected by the presence of the surface trap (to the extent that the presence of the latter induces opposite shifts of the delocalized electron and hole wave function center of mass); whereas $1/\tau_{X^-}(t_i)$, derived from the electron recombination with the surface-trapped hole, decreases, owing to the reduction in the electron−hole wave function overlap caused by the localization of the latter carrier. The other contribution affected by this is

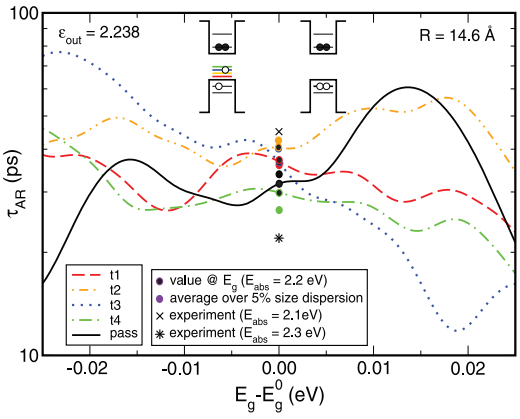

Figure 4. Auger biexciton recombination lifetimes calculated as a function of the energy difference $\varepsilon_{gap} - \varepsilon_{gap}^0$ (where ε_{gap}^0 is the value of the NC gap for a 0% size dispersion) for ε_{out} = 2.238: the carriers are either all delocalized in the dot core (XX, black solid line), or one of the holes is trapped in one of the four surface states considered (XX_s: t_1, red dashed line; t_2, orange dot-dot-dashed line; t_3, blue dotted line; t_4, green dot-dashed line). The empty symbols indicate the values calculated at ε_{gap}^0 for NCs with absorption energy E_{abs} = 2.2; the solid circles represent averages over a range of energy gaps corresponding to a 5% size dispersion, typical in experimental samples (for clarity of presentation, however, a reduced energy range is displayed in the figure). The lifetimes measured for NCs with E_{abs} = 2.3 (22 ps, star) and E_{abs} = 2.1 (45 ps, cross)[15,26] are also shown for comparison.

τ_h (the hole component in eq 1), which can become larger than for $h_j = h_1$. The magnitude of the variation of both components, however, depends on the NC size, the depth of the hole trap involved, and the value of ε_{out}: the largest effect is found for ε_{out} = 1, where $1/\tau_{X^-}(h_1)$ and $1/\tau_{X^-}(t_i)$ can differ by more than 1 order of magnitude, whereas for ε_{out} = 2.238, the difference can be minimal. As a consequence, the AR lifetimes of XX a nd XX_s can be very close for specific traps and particular values of the dielectric environment. The results presented in Figure 3 also clarify why the AR lifetimes in CdSe NCs were found[15,26] not to be significantly affected by different surface passivations.

The excellent agreement with experiment[15] (black lines in Figure 3a) obtained for ε_{out} = 2.238 (a value appropriate for toluene and most organic capping groups) for both sizes considered seems to suggest a low dielectric environment for the NC. It is interesting to point out, however, that for four core-delocalized carriers (XX), the variation of the AR lifetime with the different values of ε_{out} considered here is very small for small NCs absorbing at about 2.2 eV (less than a factor of 2 from its value at 2.238), yielding $\tau_{XX} = 44.85 \pm 13.15$ ps (for $\varepsilon_{out} > 1$), in agreement with experiment[15,26] ($22 \le \tau_{XX}^{exp} \le 45$ ps, for samples with $2.3 \ge E_{abs} \ge 2.1$ eV). Although such a variation is larger for the NC absorbing at ∼2.07 eV, the value $\tau_{XX} = 150 \pm 105$ ps that covers the same range of screening constants is still in reasonable agreement with experiment ($45 \le \tau_{XX}^{exp} \le 147$ ps for samples with $2.1 \ge E_{abs} \ge 2.0$ eV).

Another characteristic feature that could influence the measured decay lifetimes in real samples is their polydispersity. By calculating the lifetime as a function of the energy gap ε_{gap} (Figure 4), the importance of size heterogeneity was investigated: a 5% size dispersion, typically achieved experimentally (solid circles in Figure 4), was found to have negligible effects for low values of the screening on the AR lifetimes of both XX and XX_s, whereas it was found to affect the lifetimes by up to a factor of 2.3 for larger values of ε_{out}. An example is shown in Figure 4, where the AR lifetimes of XX and XX_s calculated using $\varepsilon_{out} = 2.238$ are displayed as a function of the energy difference $\varepsilon_{gap} - \varepsilon^0_{gap}$ (where ε^0_{gap} is the value of the NC gap for a 0% size dispersion). As ε_{gap} changes, the energies of initial and final states in the AR process (the denominator of eq 3) move in and out of resonance, resulting in lifetimes that oscillate around their value at ε^0_{gap} (empty circles), as illustrated by the proximity of empty and full circles, the latter representing calculated averages over a range of energy gaps corresponding to a 5% size dispersion, typical in experimental samples. The results for both 0 and 5% size distributions, relative to a NC with the first absorption peak centered around $E_{abs} = 2.26$ eV, are compared in Figure 4 with the available experimental data[15] relative to samples with $E_{abs} \sim 2.1$ ($\tau_{AR} = 45$ ps) and 2.3 eV ($\tau_{AR} = 22$ ps).[26] The agreement with experiment is excellent for both XX and XX_s and for both mono- and polydisperse samples.

The results presented here, therefore, suggest that PIST of a hole in a deep *surface* state could lead to spectroscopic signatures that can be indistinguishable from those produced by a conventional biexciton with four core-delocalized carriers and hence could be mistaken for a product of CM leading to exaggerated CM yields in static samples.

This hypothesis is also consistent with the results of earlier time-resolved PL experiments on *static* CdSe NC samples by Schaller *et al.*,[35] where CM was detected also using the spectral (as opposed to the dynamic) signatures of its products (biexcitons), confirming previous determinations based instead on transient absorption techniques.[14] In that work,[35] they showed that (i) the PL spectra collected at nominally zero delay from a low intensity, high energy excitation pulse (when CM was possible and had been detected with dynamical methods), and (ii) the early time spectra observed when biexcitons were generated using absorption of multiple photons (*i.e.*, low energy, high intensity excitations) exhibited very similar red shifts with respect to the steady-state PL spectrum of the sample (when only single excitons remain in the population of excited NCs). This was considered as an indication of the presence of biexcitons in (i) and therefore of their generation from single photons (*i.e.*, of the occurrence of CM). As the results obtained here suggest, however, the same feature could have been produced by the occurrence of PIST of a hole in a fraction of the NCs. Figure 5 shows the room temperature PL spectra calculated for X, XX, and XX_s (where $s = t_4$[36]), together with a set of spectra obtained assuming the presence of a mixture of X and XX_s in the sample, with the fraction of XX_s decreasing from 35% (the maximum CM yield that, according to an estimate by Nair and Bawendi,[12] was achieved in ref 35) to 5%. The "mixed" spectra obtained with XX_s fractions between 25 and 35% and those calculated for XX show very small relative shifts (less than 6 meV) and exhibit similar red shifts (~30 meV) from the single exciton spectrum (Figure 5, inset), with magnitudes consistent with previous measurements of biexciton binding energies,[37] whereas, as expected, increasingly smaller red shifts are obtained for decreasing XX_s content. On the basis of these results, in the absence of CM, the spectral features observed in ref 35 could have been produced by the occurrence of PIST in ~30% of the NCs, following low intensity, high energy excitation. The spectral signatures of the latter, being almost indistinguishable from those produced by conventional biexcitons, could be mistaken for evidence of CM. Furthermore, their dynamical signatures would result in an apparent CM quantum yield of ~30%. This value is in remarkable agreement with the CM yield estimated by Nair and Bawendi[12] for those samples.

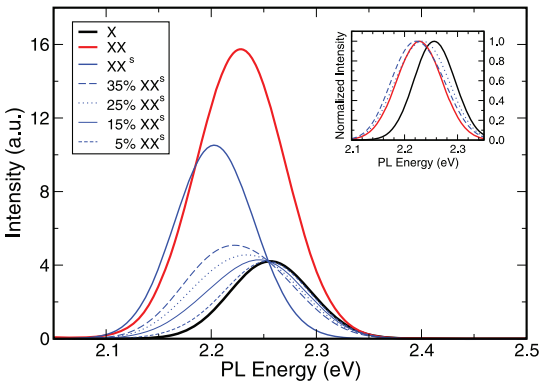

Figure 5. Calculated room temperature PL spectra for X (black solid line), XX (red solid line), and XX_s (where $s = t_4$, blue solid line), together with four spectra obtained assuming the presence of a mixture of X and XX_s in the sample, with the fraction γ of XX_s decreasing from 35% (the maximum CM yield estimated by Nair and Bawendi[12] from the data in ref 35, blue long-dashed line) to 5% (blue short-dashed line). The emission spectra of XX and $XX_s^{\gamma} + X^{(1-\gamma)}$ show relative shifts of less than 6 meV for $0.25 \leq \gamma \leq 0.35$ and exhibit similar red shifts from the single exciton spectrum. This is shown more clearly in the inset, where the intensities have been normalized to 1 for all spectra, according to the convention adopted in Figure 4 of ref 35.

A different mechanism, the formation of long-lived charge-separated states in solutions of well-passivated PbSe NCs under UV excitation, was very recently proposed by McGuire *et al.*[31] as the origin of dynamical signatures that can mimic the behavior of CM, leading to discrepancies in quantitative measurements of CM

efficiencies between stirred and static PbSe NC samples. According to this hypothesis,[31] however, one of the carriers is transferred to a trap center "*in the ligand shell at an appreciable distance from the NC*" and is therefore removed from the NC. It is important here to highlight again the key difference between PIST and photocharging[13,31] and their implications: in contrast to photoionization, in the case of PIST, the NC would remain neutral overall and the AR rates would be similar to those observed in a biexciton with all core-delocalized carriers, therefore consistent with experiment.[14] In a photocharged NC instead, the PL decay signal would show, together with the biexciton signature, additional components relative to the relaxation of charged excitons and charged biexcitons, as observed in PbSe NCs,[13] but in contrast with any experimental observation reported so far for CdSe samples.[14]

The difference in carrier relaxation and trapping dynamics observed in PbSe and CdSe NCs can be understood in terms of a different "quality" of their surface passivation: while hole trapping is an accepted and established mechanism in CdSe NCs,[9,22−24,26−28] in typical oleic-acid-capped PbSe samples, this picture is inconsistent with the observed (i) high quantum yields,[33,34] (ii) small Stokes shifts,[33,34] and (iii) slow interband relaxation.[33] In particular, luminescence from deep traps was never observed[34] in PbSe NC, and no inorganic surface passivation (such as capping with a semiconductor shell) was required to obtain room temperature PL quantum yields as high as 85%.[33] Such an effective surface passivation may therefore lead to a suppression of PIST in PbSe, due to the lack of energetically suitable trap sites on the NC surface, leaving the less favorable charge transfer to the ligand shell as the only alternative. Indeed, very low photocharging probabilities for UV excitation and long lifetimes for the charge-separated states were estimated by McGuire *et al.*[31] in their PbSe NC samples.

CONCLUSIONS

In summary, the Auger recombination lifetimes were calculated for CdSe NCs in different excitonic configurations (positive and negative trions and biexcitons), including the presence of hole surface traps. The results (i) shed light on several different experimental observations; (ii) highlight the inadequacy of the photocharging hypothesis to account for the discrepancy between the carrier multiplication yields observed in CdSe NCs by different groups, by evidencing its inconsistency with experiment, where the magnitude of the fast component of the transient absorption time traces at low pump intensity and high photon energies was found to be essentially identical to that measured at high excitation intensities for photon energies well below the CM threshold (where therefore the probability of photoionization was very low), and was furthermore incompatible with the AR lifetime calculated for any trion configuration (including both three core-delocalized carriers and two core-delocalized and one surface-trapped carrier); and (iii) provide a possible explanation for the discrepancy in terms of photoinduced surface trapping, where the core becomes charged following the trapping of a hole on the surface, *but the NC remains overall neutral*, yielding AR rates that can be indistinguishable from those of core-delocalized biexcitons and resulting in exaggerated CM yields in static samples. Although this hypothesis was dismissed as unlikely for PbSe nanocrystals, in the case of CdSe, it is further supported by (a) recent femtosecond pump−probe spectroscopic measurements on CdSe nanostructures,[22] showing increased probability of surface trapping for highly excited states and very high trapped carrier fractions; (b) state-resolved transient absorption studies of biexcitonic states in CdSe NCs,[23] revealing enhanced surface trapping rates for excited exciton states, yielding biexcitons constituted by an electron and a surface-trapped hole plus the band edge exciton; (c) recent single-NC photoionization studies on CdSe core/shell NCs,[24] suggesting the creation by high energy excitations (but not by low energy, direct excitation of the emitting exciton) of charge-separated complexes, with a surface-trapped hole and a core-delocalized electron; (d) single-dot blinking studies *in the absence of illumination*,[25] finding an extremely low probability of "on−off" transitions (commonly associated with the trapping of a carrier) in the dark.

Finally, the spectral features attributed to CM in early time-resolved PL experiments have been shown to be reproduced in the absence of CM by the occurrence of PIST of a hole in ∼30% of the NCs following low intensity, high energy excitation, in remarkable agreement with the CM quantum yields estimated for those samples.

These results suggest that multicarrier processes could be mediated by different mechanisms in CdSe and PbSe NCs. The difference in their surface "quality" could explain the difference between the carrier dynamics observed in the two material systems, where a more effective surface passivation may lead to a suppression of PIST in oleic-acid-capped PbSe NCs.

COMPUTATIONAL METHODS

AR lifetimes were calculated using the formalism developed in ref 16, where the biexciton AR rate $1/\tau_{XX}$ can be separated into an electron ($1/\tau_e$) and a hole ($1/\tau_h$) component according to

$$\frac{1}{\tau_{XX}} = \frac{1}{\tau_e} + \frac{1}{\tau_h} \quad (1)$$

The latter are related to the trion decay rates by

$$\frac{1}{\tau_e} = \frac{1}{\tau_{X^-}(h_1)} + \frac{1}{\tau_{X^-}(h_j)} \quad (2a)$$

$$\frac{1}{\tau_h} = \frac{2}{\tau_{X^+}(h_1, h_j)} \quad (2b)$$

where $h_j = h_1$ (*i.e.*, the ground state hole) or $h_j = t_i$ (the trap state), depending on the configuration, and the trion decay rates are expressed as

$$\frac{1}{\tau_{X^-}(h_1)} = \frac{\Gamma}{\hbar}\sum_n \frac{|J(e_{1,\uparrow}, e_{1,\downarrow}; e_n, h_1) - J(e_{1,\downarrow}, e_{1,\uparrow}; e_n, h_1)|^2}{(\varepsilon_{gap} - \varepsilon_{e_n} + \varepsilon_{e_1})^2 + (\Gamma/2)^2} \quad (3a)$$

$$\frac{1}{\tau_{X^+}(h_1, h_1)} = \frac{\Gamma}{\hbar}\sum_n \frac{|J(h_{1,\uparrow}, h_{1,\downarrow}; h_n, e_1) - J(h_{1,\downarrow}, h_{1,\uparrow}; h_n, e_1)|^2}{(\varepsilon_{gap} + \varepsilon_{h_n} - \varepsilon_{h_1})^2 + (\Gamma/2)^2} \quad (3b)$$

Here the subscripts ↑ and ↓ indicate the spin-degenerate Kramer's doublets, $\varepsilon_{gap} = \varepsilon_{e_1} - \varepsilon_{h_1}$ is the single-particle energy gap, and

$$J(j,k,l,m) = \sum_{\sigma,\sigma'} \int\int \phi_j^*(\mathbf{r},\sigma)\phi_k^*(\mathbf{r}',\sigma')\frac{e^2}{\varepsilon(\mathbf{r},\mathbf{r}')|\mathbf{r}-\mathbf{r}'|} \times \phi_l(\mathbf{r},\sigma)\phi_m(\mathbf{r}',\sigma')d^3r d^3r' \quad (4)$$

where $\{\phi_i\}$ are the single-particle wave functions, calculated using the plane-wave semiempirical pseudopotential method described in ref 18, including spin−orbit effects; τ_{X^-} and τ_{X^+} were calculated including all states within an energy window of ∼100 meV, centered around the ideal energy $\varepsilon_{gap^*} + \varepsilon_{e_1}$ and $\varepsilon_{gap^*} - \varepsilon_{h_1}$, respectively (where $\varepsilon_{gap^*} = \varepsilon_{e_1} - \varepsilon_{h_1}$). Surface states t_i (with $i = 1,...,4$ increasing with depth, from an energy $\varepsilon_{t_1} \approx \varepsilon_{h_1} +$ 170 meV to $\varepsilon_{t_4} \approx \varepsilon_{h_1} +$ 580 meV), where the hole has different degrees of overlap with the electron wave function, were created by unpassivating surface Se atoms according to the procedure detailed in ref 19.

In order to account for different possible environments, including solvents, capping groups, and semiconductor shell materials, covering a variation of over 1 order of magnitude (from ∼2 to ∼30), in the dielectric constant, the regional screening developed in ref 16 was used, where the microscopic dielectric function of the dot is expressed in terms of a core and a surface term as

$$\varepsilon^{-1}(\mathbf{r},\mathbf{r}') = \varepsilon_{out}^{-1}(\mathbf{r},\mathbf{r}') + (\varepsilon_{in}^{-1}(\mathbf{r},\mathbf{r}') - \varepsilon_{out}^{-1}(\mathbf{r},\mathbf{r}'))m(r)m(r') \quad (5)$$

In eq 5, $m(r)$ changes smoothly from 1, when r is inside the dot ($r < R_{dot} - d$), to 0, when r is outside ($r > R_{dot} + d$), yielding $\varepsilon(\mathbf{r},\mathbf{r}') = \varepsilon_{in}$ inside the dot, while $\varepsilon(\mathbf{r},\mathbf{r}') = \varepsilon_{out}$ when r, r', or both are outside the dot (here d is chosen to be 2 Å). In this work, ε_{in} was assumed to be equal to its bulk value, whereas ε_{out} was chosen equal to 1, 2.238, 6, 8.5, and 12.5 to represent as wide as possible a range of dielectric constant values of realistic materials that can be present at the dot surface.

Acknowledgment. Part of the results presented in this work was obtained using the UK National Grid Service (NGS). Financial support from the Royal Society under the URF scheme is gratefully acknowledged.

REFERENCES AND NOTES

1. Becerra, L. R.; Murray, C. B.; Griffin, R. G.; Bawendi, M. G. Investigation of the Surface Morphology of Capped CdSe Nanocrystallites by ^{31}P Nuclear Magnetic Resonance. *J. Chem. Phys.* **1994**, *100*, 3297–3300.
2. Kuno, M.; Lee, J. K.; Dabbousi, B. O.; Mikulec, F. V.; Bawendi, M. G. The Band Edge Luminescence of Surface Modified CdSe Nanocrystallites: Probing the Luminescing State. *J. Chem. Phys.* **1997**, *106*, 9869–9882.
3. Kalyuzhny, G.; Murray, R. W. Ligand Effects on Optical Properties of CdSe Nanocrystals. *J. Phys. Chem. B* **2005**, *109*, 7012–7021.
4. Guyot-Sionnest, P.; Wehrenberg, B.; Yu, D. Intraband Relaxation in CdSe Nanocrystals and the Strong Influence of the Surface Ligands. *J. Chem. Phys.* **2005**, *123*, 074709-1–074709-7.
5. Bawendi, M. G.; Carroll, P. J.; Wilson, W. L.; Brus, L. E. Luminescence Properties of CdSe Quantum Crystallites: Resonance between Interior and Surface Localized States. *J. Chem. Phys.* **1992**, *96*, 946–954.
6. Underwood, D. F.; Kippeny, T.; Rosenthal, S. Ultrafast Carrier Dynamics in CdSe Nanocrystals Determined by Femtosecond Fluorescence Upconversion Spectroscopy. *J. Phys. Chem. B* **2001**, *105*, 436–443.
7. Myung, N.; Ding, Z.; Bard, A. J. Electrogenerated Chemiluminescence of CdSe Nanocrystals. *Nano Lett.* **2002**, *2*, 1315–1319.
8. Lifshitz, E.; Glozman, A.; Litvin, I. D.; Porteanu, H. Optically Detected Magnetic Resonance Studies of the Surface/Interface Properties of II−VI Semiconductor Quantum Dots. *J. Phys. Chem. B* **2000**, *104*, 10449–10461.
9. Gomez, D. E.; Califano, M; Mulvaney, P. Optical Properties of Single Semiconductor Nanocrystals. *Phys. Chem. Chem. Phys.* **2006**, *8*, 4989–5011.
10. Myung, N.; Bae, Y.; Bard, A. J. Effect of Surface Passivation on the Electrogenerated Chemiluminescence of CdSe/ZnSe Nanocrystals. *Nano Lett.* **2003**, *3*, 1053–1055.
11. Schaller, R. D.; Klimov, V. I. High Efficiency Carrier Multiplication in PbSe Nanocrystals: Implications for Solar Energy Conversion. *Phys. Rev. Lett.* **2004**, *92*, 186601-1–186601-4.
12. Nair, G.; Bawendi, M. G. Carrier Multiplication Yields of CdSe and CdTe Nanocrystals by Transient Photoluminescence Spectroscopy. *Phys. Rev. B* **2007**, *76*, 081304-1–081304-4.
13. McGuire, J. A.; Sykora, M.; Joo, J.; Pietryga, J. M.; Klimov, V. I. Apparent *versus* True Carrier Multiplication Yields in Semiconductor Nanocrystals. *Nano Lett.* **2010**, *10*, 2049–2057.
14. Schaller, R. D.; Petruska, M. A.; Klimov, V. I. Effect of Electronic Structure on Carrier Multiplication Efficiency: Comparative Study of PbSe and CdSe Nanocrystals. *Appl. Phys. Lett.* **2005**, *87*, 253102-1–253102-3.
15. Klimov, V. I.; Mikhailovsky, A. A.; McBranch, D. W.; Leatherdale, C. A.; Bawendi, M. G. Quantization of Multiparticle Auger Rates in Semiconductor Quantum Dots. *Science* **2000**, *287*, 1011–1013.
16. Wang, L.-W.; Califano, M.; Zunger, A.; Franceschetti, A. Pseudopotential Theory of Auger Processes in CdSe Quantum Dots. *Phys. Rev. Lett.* **2003**, *91*, 056404-1–056404-4.
17. Only one deep surface state (T_1, with $\varepsilon_{T_1} \approx \varepsilon_{h_1} +$ 510 meV) was considered for the 19.2 Å NC.
18. Wang, L.-W.; Zunger, A. Local-Density-Derived Semiempirical Pseudopotentials. *Phys. Rev. B* **1995**, *51*, 17398–17416.
19. Califano, M. Efficient Auger Electron Cooling in Seemingly Unfavorable Configurations: Hole Traps and Electrochemical Charging. *J. Phys. Chem. C* **2008**, *112*, 8570–8574.
20. Califano, M. Direct and Inverse Auger Processes in InAs Nanocrystals: Can the Decay Signature of a Trion be Mistaken for Carrier Multiplication?. *ACS Nano* **2009**, *3*, 2706–2714.
21. Jha, P. P.; Guyot-Sionnest, P. Trion Decay in Colloidal Quantum Dots. *ACS Nano* **2009**, *3*, 1011–1015.
22. Cretí, A.; Anni, M.; Zavelani Rossi, M.; Lanzani, G.; Leo, G.; Della Sala, F.; Manna, L.; Lomascolo, M. Ultrafast Carrier Dynamics in Core and Core/Shell CdSe Quantum Rods: Role of the Surface and Interface Defects. *Phys. Rev. B* **2005**, *72*, 125346-1–125346-10.
23. Sewall, S. L.; Cooney, R. R.; Anderson, K. E. H.; Dias, E. A.; Sagar, D. M.; Kambhampati, P. State-Resolved Studies of Biexcitons and Surface Trapping Dynamics in Semiconductor Quantum Dots. *J. Chem. Phys.* **2008**, *129*, 084701-1–084701-8.

24. Li, S; Steigerwald, L.; Brus, L. E. Surface States in the Photoionization of High-Quality CdSe Core/Shell Nanocrystals. *ACS Nano* **2009**, *3*, 1267–1273.
25. Baker, T. A.; Rouge, J. L.; Nesbitt, D. J. Single Molecule studies of Quantum Dot Fluorescence Intermittency: Evidence for Both Dark and Light-Assisted Blinking Dynamics. *Mol. Phys.* **2009**, *107*, 1867–1878.
26. Klimov, V. I. Optical Nonlinearities and Ultrafast Carrier Dynamics in Semiconductor Nanocrystals. *J. Phys. Chem. B* **2000**, *104*, 6112–6123.
27. Klimov, V. I.; Schwarz, C. J.; McBranch, D. W.; Leatherdale, C. A.; Bawendi, M. G. Ultrafast Dynamics of Inter- and Intraband Transitions in Semiconductor Nanocrystals: Implications for Quantum-Dot Lasers. *Phys. Rev. B* **1999**, *60*, R2177–R2180.
28. Klimov, V. I.; Mikhailovsky, A. A.; McBranch, D. W.; Leatherdale, C. A.; Bawendi, M. G. Mechanisms for Intraband Energy Relaxation in Semiconductor Quantum Dots: The Role of Electron−Hole Interactions. *Phys. Rev. B* **2000**, *61*, R13349–R13352.
29. Klimov, V. I.; McBranch, D. W. Femtosecond 1P-to-1S Electron Relaxation in Strongly Confined Semiconductor Nanocrystals. *Phys. Rev. Lett.* **1998**, *80*, 4028–4031.
30. Frantsuzov, P. A.; Marcus, R. A Explanation of Quantum Dot Blinking without the Long-Lived Trap Hypothesis. *Phys. Rev. B* **2005**, *72*, 155321-1–155321-10.
31. McGuire, J. A.; Sykora, M.; Robel, I.; Padilha, L. A.; Joo, J.; Pietryga, J. M.; Klimov, V. I. Spectroscopic Signatures of Photocharging Due to Hot-Carrier Transfer in Solutions of Semiconductor Nanocrystals under Low-Intensity Ultraviolet Excitation. *ACS Nano* **2010**, *4*, 6087–6097.
32. Pandey, A.; Guyot-Sionnest, P. Multicarrier Recombination in Colloidal Quantum Dots. *J. Chem. Phys.* **2007**, *127*, 111104-1–111104-4.
33. Wehrenberg, B. L.; Wang, C.; Guyot-Sionnest, P. Interband anad Intraband Optical Studies of PbSe Colloidal Quantum Dots. *J. Phys. Chem. B* **2002**, *106*, 10634–10640.
34. Du, H.; Chen, C.; Krishnan, R.; Krauss, T. D.; Harbold, J. M.; Wise, F. W.; Thomas, M. G.; Silcox, J. Optical Properties of Colloidal PbSe Nanocrystals. *Nano Lett.* **2002**, *2*, 1321–1324.
35. Schaller, R. D.; Sykora, M.; Jeong, S.; Klimov, V. I. High-Efficiency Carrier Multiplication and Ultrafast Charge Separation in Semiconductor Nanocrystals Studied *via* Time-Resolved Photoluminescence. *J. Phys. Chem. B* **2006**, *110*, 25332–25338.
36. Similar results were obtained for the other surface states considered in this work.
37. Achermann, M.; Hollingsworth, J. A.; Klimov, V. I. Multiexcitons Confined within a Subexcitonic Volume: Spectroscopic and Dynamical Signatures of Neutral and Charged Biexcitons in Ultrasmall Semiconductor Nanocrystals. *Phys. Rev. B* **2003**, *68*, 245302-1–245302-5.